

Rolled Gaussian process models for curves on manifolds

S. P. Preston^{1*}, K. Bharath¹, P. C. López-Custodio², A. Kume³

Abstract

Given a planar curve, imagine rolling a sphere along that curve without slipping or twisting, and by this means tracing out a curve on the sphere. It is well known that such a rolling operation induces a local isometry between the sphere and the plane so that the two curves uniquely determine each other, and moreover, the operation extends to a general class of manifolds in any dimension. We use rolling to construct an analogue of a Gaussian process on a manifold starting from a Euclidean Gaussian process. The resulting model is generative, and is amenable to statistical inference given data as curves on a manifold. We illustrate with examples on the unit sphere, symmetric positive-definite matrices, and with a robotics application involving 3D orientations.

1 Introduction

1.1 Background and motivation

Many modern applications generate data where the statistical unit is a curve on a manifold, M . An interesting example is robotics: in a given task, a robot arm’s end-effector traces a curve in a space of orientations. We consider one such example later, with data as smooth curves $t \mapsto x(t) \in M$, where M is the manifold of rotation matrices. Despite prevalence of such data [e.g. Su et al., 2014, Zhang et al., 2018], there is a dearth of suitable generative and statistical models that are simple and tractable.

For curves in a Euclidean space, \mathbb{R}^d , Gaussian processes offer an appealing model due to their characterization by a mean and a covariance function, computational tractability, and closure under marginalization and conditioning. However, Gaussian processes rely on covariance operators defined using the global vector space structure of \mathbb{R}^d , which is absent on a d -dimensional nonlinear M . Having an analogue of a Gaussian process on M will facilitate modelling and inference of manifold-valued curve data. A key objective of this paper is to define such a process.

A strategy to address manifold nonlinearity is to consider a mapping between M and \mathbb{R}^d , enabling a curve on M to be identified with a curve on \mathbb{R}^d and vice versa; these are respectively “flattening” and “unflattening” maps. Pairing a generative model for curves in \mathbb{R}^d with suitable unflattening maps provides a generative model for curves on M . In the other direction, for inference given observed data that are curves on M , the flattening maps facilitate practical computations and statistical inference for the model parameters. We follow this strategy: for the model in \mathbb{R}^d we use the Gaussian process, for unflattening we use a pair of maps termed “rolling” and “wrapping”, and for flattening we use a reverse pair of maps termed “unrolling” and “unwrapping”. We define

¹School of Mathematical Sciences, University of Nottingham, UK

²Computer Science Department, Nottingham Trent University, UK

³School of Mathematics, Statistics and Actuarial Science, University of Kent, UK

*simon.preston@nottingham.ac.uk

these four maps precisely below.

The four maps are compatible with the intrinsic geometry of M , do not introduce any distortions, and are optimal in a sense clarified below. This is in contrast to identifying \mathbb{R}^d with a tangent space at a single fixed point on M , and using tangent space projections between the tangent space and M , and vice versa, which causes distortions. Our maps provide a natural way to define a covariance, and hence a Gaussian process model, on M , starting with one in \mathbb{R}^d .

1.2 Related works, and contributions

“Rolling” of a curve in \mathbb{R}^d onto M , and its reverse operation, “unrolling”, originate from mathematical geometry, where they are known as *antidevelopment* and *development* respectively; see Kobayashi and Nomizu [1996] and Sharpe [2000]. Jupp and Kent [1987] first exploited the idea in statistics, to define smoothing curves for time-indexed data points on the unit sphere. Kume et al. [2007] adapted their technique to shape spaces, and later Kim et al. [2021] generalized to Riemannian manifolds. These works, however, did not consider statistical models for inference.

The notion of stochastic development has been used to define generative diffusion models for curves on M [e.g. Sommer, 2019, 2020] based on stochastic differential equations in \mathbb{R}^d . Markovian property of the models do not allow for rich covariance structures, and computational challenges abound: exact simulation is infeasible, numerical approximations are costly, and likelihood functions lack closed-form expressions, complicating inference.

Notions of covariance of a random curve x on M with respect to a fixed curve γ have been considered. The extrinsic approach by Dai and Müller [2019] for embedded submanifolds M results in a covariance that depends on the embedding. To define an intrinsic covariance operator of a random vector field along γ , Lin and Yao [2019] used the tensor Hilbert space of tangent spaces along γ , while Shao et al. [2022] used an abstract notion of a covariance bundle. The common focus of these papers is on principal component analysis with γ as the Fréchet mean curve, albeit under different sampling regimes, and models for inference were not considered. Methodology for curves with values in a general metric space that do not explicitly use the differentiable structure of the manifold M have been developed [Dubey and Müller, 2020, 2022].

Mallasto and Feragen [2018] defined a model for x on M by wrapping, under the exponential map, a Gaussian vector field along a mean curve γ with covariance as in Lin and Yao [2019]. A similar approach was adopted recently by Liu et al. [2024] and Wang et al. [2024]. The issue with using such models for inference is two-fold: as with \mathbb{R}^d -valued Gaussian processes, the mean curve γ and the covariance have to be jointly estimated; however, the strategies used in \mathbb{R}^d , such as using a basis representation for x , or a parametric covariance structure, are difficult to devise. In the above works, the mean function is either pre-specified or estimated separately.

The main contributions of this paper are: (i) to use rolling and wrapping with respect to coordinate frames to specify how a Gaussian process model in \mathbb{R}^d can be identified with a “rolled Gaussian process” model on M , while establishing its invariances and equivariances to choice of frames; (ii) to establish conditions for the Fréchet mean of the rolled Gaussian process model to equal the rolling of the mean of the Gaussian process in \mathbb{R}^d ; (iii) to prescribe a finite-dimensional parameterisation of the rolled Gaussian process model, with statistical estimators and tests for the model parameters, in the practically useful setting when sample curves are observed at a finite set of times; and (iv) to establish conditions under which estimators of the parameters defining the mean curve consistently estimate their population counterpart. The technical contributions in (ii) concerning the interplay between notions of symmetry of the manifold and a distribution, and in (iv) on convergence of parallel transport maps along a sequence of random curves to their counterparts along the limiting curve, may be of independent interest.

2 Preliminaries

We record relevant definitions from Riemannian geometry and geometric statistics, and refer to Kobayashi and Nomizu [1996], Lee [2018] and Pennec et al. [2019], respectively, for details.

Let M be a complete connected Riemannian manifold of dimension d . Denote by T_pM the tangent space at each point $p \in M$ and by $TM = \{T_pM : p \in M\}$ the collection of tangent spaces, known as the tangent bundle. On the tangent space T_pM at each point p , we can define an inner product $\langle \cdot, \cdot \rangle_p : T_pM \times T_pM \rightarrow \mathbb{R}_{\geq 0}$ with induced norm $\| \cdot \|_p$; the collection $\{\langle \cdot, \cdot \rangle_p : p \in M\}$ is referred to as a Riemannian metric. The Riemannian metric varies smoothly along the manifold and allows us to measure distances, volumes, and angles.

For a curve $\gamma : [0, 1] \rightarrow M$, its velocity at t is $\dot{\gamma}(t) := d\gamma(t)/dt \in T_{\gamma(t)}M$, and its length $L(\gamma)$ is the scalar $\int_0^1 \|\dot{\gamma}(t)\|_{\gamma(t)}^{1/2} dt$. For all curves in this paper, the parameter domain is the unit interval, $[0, 1]$. Often, but not always, t is interpreted as time; we refer to it thus in the following.

The Riemannian metric g defines a unique affine connection called the Levi-Civita connection ∇ , known as the covariant derivative, which describes how vectors in tangent spaces change as one moves along a curve γ from one point to another. A vector field $t \mapsto V(t) \in T_{\gamma(t)}M$ along a curve γ is said to be parallel if $\nabla_{\dot{\gamma}(t)}V(t) = 0$ for all t . Given a curve $\gamma : [0, 1] \rightarrow M$ and $u \in T_{\gamma(t_0)}M$ for $t_0 \in [0, 1]$, there exists a unique parallel vector field V such that $V(t_0) = u$.

Vectors in different tangent spaces are identified using *parallel transport* along a curve γ : the parallel transport of $u \in T_{\gamma(s)}M$ along γ to $T_{\gamma(t)}M$ is $V(t)$, where V is the unique parallel vector field determined by $V(s) = u$. This engenders a linear isometry $P_{t \leftarrow s}^\gamma : T_{\gamma(s)}M \rightarrow T_{\gamma(t)}M$, $P_{t \leftarrow s}^\gamma(u) = V(t)$, between tangent spaces at points along γ , such that $\langle u, w \rangle_{\gamma(s)} = \langle P_{t \leftarrow s}^\gamma(u), P_{t \leftarrow s}^\gamma(w) \rangle_{\gamma(t)}$ for every u, w ; its inverse is denoted by $P_{s \leftarrow t}^\gamma$.

Curves γ with zero acceleration such that $\nabla_{\dot{\gamma}(t)}\dot{\gamma}(t) = 0$ for all t are called *geodesics*. The distance ρ between points p and q is the length of a segment of a geodesic curve connecting the two, known as the minimal geodesic: $\rho(p, q) = \inf\{L(\gamma) | \gamma : [0, 1] \rightarrow M; \gamma(0) = p, \gamma(1) = q\}$.

Given a point p and a geodesic γ with $\gamma(0) = p$, a cut point of p is defined as the point $\gamma(t_0)$ such that γ is a minimal geodesic on the interval $[0, t_0]$ but fails to be for $t > t_0$. The set of cut points of geodesics starting at p is its *cut locus* $\mathcal{C}(p)$. The injectivity radius of p is its distance to $\mathcal{C}(p)$, and the injectivity radius $i(M)$ of M is the infimum of the injectivity radii of points in M .

The next two tools are necessary for moving between M and its tangent spaces. Geodesics on M are used to define the *exponential map* $\exp : TM \rightarrow M$, which maps a point (p, v) in the tangent bundle to a point on M ; in particular, when restricted to T_pM it is defined via a geodesic $\gamma : [0, 1] \rightarrow M$ starting at $\gamma(0) = p$ with initial velocity $\dot{\gamma}(0) = v$ as $\exp_p : T_pM \rightarrow M, \exp_p(v) = \gamma(1)$. From the Hopf-Rinow theorem, on a complete manifold the exponential map is surjective. On an star shape region around the origin in T_pM it is a diffeomorphism onto its image outside of the cut locus of p , and a well-defined inverse $\exp_p^{-1} : M \rightarrow T_pM$ exists, known as the *inverse exponential* or logarithm map, that maps a point on M outside of $\mathcal{C}(p)$ to T_pM ; thus for any q outside of $\mathcal{C}(p)$, $\rho(p, q) = \|\exp_p^{-1}(q)\|_p$. Relatedly, the *tangent cut locus* $\mathcal{T}(p) \subset T_pM$ of $p \in M$, is defined by the relation $\exp_p(\mathcal{T}(p)) = \mathcal{C}(p)$.

There are many notions of curvature of a Riemannian manifold. We will mainly be concerned with *sectional curvature* at a point p , defined to be the Gaussian curvature at p of the two-dimensional surface swept out by the set of all geodesics starting at p with initial velocities lying in the two-dimensional subspace of T_pM spanned by two linear independent vectors. Throughout, we will simply use curvature to mean sectional curvature, and describe a manifold M as positively (non-positively) curved if its curvature at every point is positive (non-positive). Non-positively curved M have infinite $i(M)$ with empty cut locus such that $\exp_p : T_pM \rightarrow M$ is a global diffeomorphism at every p .

The *Fréchet mean* of a probability measure ν on M is defined as the minimizer of

$$y \mapsto \int_M \rho^2(y, x) d\nu(x); \quad (2.1)$$

sufficient conditions that ensure existence and uniqueness of the Fréchet mean on manifolds are well-known [e.g. Afsari, 2011]. When ν is the empirical measure of a sample of points in M , the minimizer is the *sample Fréchet mean*. Under suitable conditions the sample Fréchet mean converges almost surely to its population counterpart [Ziezold, 1977]. Abusing terminology, we also speak of the Fréchet mean of a random variable x where $x \sim \nu$; context will disambiguate the two. For a random curve $x : [0, 1] \rightarrow M$ the *population Fréchet mean curve*, $\gamma_{\text{Fre}} : [0, 1] \rightarrow M$, is defined as the Fréchet mean of x pointwise in t ; that is,

$$\gamma_{\text{Fre}}(t) = \operatorname{argmin}_{s \in M} E\{\rho^2(x(t), s)\}. \quad (2.2)$$

For a sample of curves, $\{x_1, \dots, x_n\}$, the *sample Fréchet mean curve* is $\hat{\gamma}_{\text{Fre}} : [0, 1] \rightarrow M$,

$$\hat{\gamma}_{\text{Fre}}(t) := \operatorname{argmin}_{s \in M} \frac{1}{n} \sum_{i=1}^n \rho^2(x_i(t), s). \quad (2.3)$$

We will refer to a special class of manifolds known as symmetric manifolds when describing the relationship between the pointwise Fréchet mean curve and a mean curve under our proposed model. A *symmetric manifold* is a manifold M in which for every $p \in M$ there is a unique isometry $\sigma_p : M \rightarrow M$ such that on $T_p M$ its differential, $d\sigma_p = -\text{id}$, the negative of the identity map; thus, σ_p reverses geodesics γ through p so that if $\gamma(0) = p$, then $\sigma_p(\gamma(t)) = \gamma(-t)$. A function $g : M \rightarrow \mathbb{R}$ on a symmetric manifold M is said to be *symmetric* if $g(p) = g(\sigma_p(p))$ for every $p \in M$. Relatedly, a distribution ν on M is said to possess *even symmetry* about $p \in M$, when $\nu = (\exp_p)_\# \lambda$, the pushforward under the exponential map at p of a mean-zero distribution λ on $T_p M$ with Lebesgue density f , when $T_p M$ is identified with \mathbb{R}^d , satisfies $f(v) = f(-v)$ for every $v \in T_p M$. More generally, the measure ν on M defined as a pushforward under the exponential map of a measure on $T_p M$ is commonly referred to as a *wrapped distribution* on M .

3 Rolled models for curves on M

3.1 Four maps for curves: unrolling, rolling, unwrapping, and wrapping

Prior to defining the four maps for curves, we introduce some preparatory notation and definitions. The *unrolling into the tangent space* of $\gamma(0)$ of a piecewise smooth curve $\gamma : [0, 1] \rightarrow M$ is the unique curve $\gamma^\downarrow : [0, 1] \rightarrow T_{\gamma(0)}(M)$ with $\gamma^\downarrow(0) = 0$, determined by the differential equation

$$\dot{\gamma}^\downarrow(t) = P_{0 \leftarrow t}^\gamma \dot{\gamma}(t). \quad (3.1)$$

Conversely, γ on M is determined by γ^\downarrow , and we refer thus to γ as the *rolling* of the curve γ^\downarrow from $T_{\gamma(0)}(M)$ onto M . Uniqueness of the parallel transport maps along γ in (3.1) [Theorem 4.32, Lee, 2018] ensures that the unrolling and rolling operations are well-defined, and are inverses of each other. Figure 1(a) provides an illustration of the unrolling of a piecewise geodesic curve on \mathbb{S}^2 onto the tangent space of its initial point. The process of unrolling has an intuitive physical analogy [Jupp and Kent, 1987]: imagine that the curve $\gamma : [0, 1] \rightarrow \mathbb{S}^2$ on the unit 2-sphere \mathbb{S}^2 is drawn in wet ink; its unrolling onto the plane \mathbb{R}^2 , when identified with $T_{\gamma(0)} M$, is the trace of the wet ink left on \mathbb{R}^2 upon rolling \mathbb{S}^2 along γ on \mathbb{R}^2 without slipping and twisting. Slipping and twisting is avoided by use of the parallel transport maps, which ensure that the tangent vectors $\dot{\gamma}(t)$ and $\dot{\gamma}^\downarrow(t)$ line up at each t .

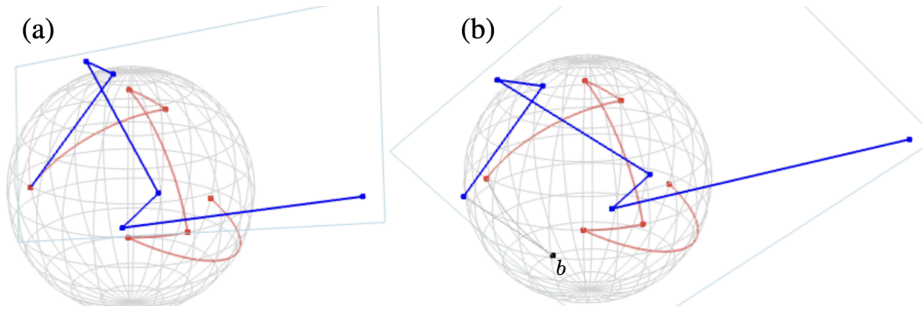


Figure 1: A piecewise geodesic curve γ on \mathbb{S}^2 , red, and its unrolling, blue, into a piecewise linear curve; (a) shows the unrolling γ^\downarrow into the tangent space $T_{\gamma(0)}\mathbb{S}^2$ at the initial point of the curve, and (b) shows the unrolling γ_b^\downarrow , incorporating a translation shown in grey, into the tangent space, T_b , at a prescribed point, b . Unrolling, and its inverse, rolling, preserve consecutive inter-point distances on γ and γ^\downarrow .

For piecewise geodesic curves, as in the example in Figure 1, a key feature of unrolling, and hence also of the rolling, is that tangent directions and distance between consecutive points along γ are preserved in γ^\downarrow , and vice versa. In contrast, a global flattening strategy by projecting the entire curve γ onto $T_{\gamma(0)}M$ via the inverse exponential map would distort distances between consecutive points in its image $\exp_{\gamma(0)}^{-1}(\gamma)$ relative to their distances in γ ; there is thus no such distortion associated with the unrolling operation. For modelling purposes, therefore, a mean curve on M may be conveniently defined as the rolling of a curve prescribed on a tangent space.

To define a suitable covariance, we require a sensible notion of deviation of a curve x on M from another fixed curve γ on M that is compatible with the rolling/unrolling operations. To begin with, we consider the deviation of a *point*, x , that is associated with with $t \in [0, 1]$. Accordingly, given a curve $\gamma : [0, 1] \rightarrow M$, the *unwrapping of point* x , assumed to be outside the cut locus $\mathcal{C}\{\gamma(t)\}$ of $\gamma(t)$, onto $T_{\gamma(0)}M$ defined as

$$(t, x) \mapsto P_{0 \leftarrow t}^\gamma \left\{ \exp_{\gamma(t)}^{-1}(x) \right\} \in T_{\gamma(0)}M. \quad (3.2)$$

The reverse operation, for a point y on $T_{\gamma(0)}M$ associated with $t \in [0, 1]$ is the *wrapping of point* $y \in T_{\gamma(0)}M$ onto M with respect to the curve γ :

$$(t, y) \mapsto \exp_{\gamma(t)}(P_{t \leftarrow 0}^\gamma y) \in M. \quad (3.3)$$

Given a curve γ on M , wrapping and unwrapping operations are inverses of each other outside of $\mathcal{C}(\gamma(0))$.

Definition 3.1. Two curves x and y are said to be “outside the cut loci of each other” if for every t , $x(t)$ lies outside of $\mathcal{C}\{y(t)\}$, the cut locus of $y(t)$.

It is possible to wrap an entire curve onto M , and not just a point, with respect to a fixed curve γ , by applying (3.3) pointwise for every $t \in [0, 1]$. The same applies to unwrapping of a curve x with respect to γ using (3.2), when x and γ are outside the cut loci of each other. Consequently, we are hence in a position to define as follows the four maps central to this paper, which map curves from a manifold to a tangent space and vice versa.

These four maps are generalizations of those defined in Kim et al. [2021] in several respects: first, rather than being defined for points, all of them map curves to curves; second, they are with respect to general curves, not necessarily piecewise geodesic curves; and third, we include a “translation”, via a parallel transport operation along a unique geodesic between b and $\gamma(0)$,

such that the “flat space” in which we work is the tangent space T_bM at some prescribed fixed point $b \in M$ —see for example Figure 1(b). This proves important later, when we take γ to play the role of the mean curve and seek to estimate it from data; the translation to T_bM means that computations are in a fixed tangent space rather than a tangent space that depends on parameters being estimated.

Definition 3.2 (The four maps). Let \mathcal{F} and \mathcal{F}_b be the space of piecewise smooth curves on M and T_bM , both with parameter domain $[0, 1]$, where $b \in M \setminus \mathcal{C}(\gamma(0))$. Let $\gamma \in \mathcal{F}$, and let $c : [0, 1] \rightarrow M$ be the geodesic from b to $\gamma(0)$.

- (a) The *unrolling* map $\mathcal{F} \rightarrow \mathcal{F}_b$ transforms a curve γ into a curve γ_b^\downarrow , with $\gamma_b^\downarrow(0) = \exp_b^{-1}\{\gamma(0)\}$, satisfying

$$\dot{\gamma}_b^\downarrow(t) = P_{0 \leftarrow 1}^c P_{0 \leftarrow t}^\gamma \dot{\gamma}(t). \quad (3.4)$$

- (b) The *rolling* map $\mathcal{F}_b \rightarrow \mathcal{F}$ is the unique inverse of the unrolling map.

- (c) The *unwrapping* map $\mathcal{F} \rightarrow \mathcal{F}_b$ transforms a curve x , with respect to another curve $\gamma \in \mathcal{F}$, into the curve

$$x_b^{\downarrow\gamma}(t) = \gamma_b^\downarrow(t) + P_{0 \leftarrow 1}^c P_{0 \leftarrow t}^\gamma \left\{ \exp_{\gamma(t)}^{-1}(x(t)) \right\}, \quad (3.5)$$

whenever x is outside the cut loci of γ .

- (d) The *wrapping* map $\mathcal{F}_b \rightarrow \mathcal{F}$ transforms a curve y , with respect to another curve $\gamma \in \mathcal{F}$, into the curve

$$y_b^{\uparrow\gamma}(t) = \exp_{\gamma(t)} \left[P_{t \leftarrow 0}^\gamma P_{1 \leftarrow 0}^c \left\{ y(t) - \gamma_b^\downarrow(t) \right\} \right]. \quad (3.6)$$

Remark 3.1. Unwrapping of a curve x on M with respect to γ on M can be viewed as a two-step process: (i) obtain the vector field along γ pointing towards x via the inverse exponential map $\exp_{\gamma(t)}^{-1}(x(t))$; (ii) apply the unrolling map in Definition 3.2(a) to the integral curve of this vector field, and translate to a new origin in T_bM . Consequently, the unwrapping map reduces to the unrolling map when $x = \gamma$ in (3.5); in other words, the unwrapping of a curve with respect to itself is its unrolling.

Remark 3.2. Provided x in (c) is outside the cut loci of γ , the wrapping map is the unique inverse of the unwrapping map. Provided y in (d) is such that the argument of $\exp_{\gamma(t)}$ in (3.6) is outside the tangential cut locus $\mathcal{T}\{\gamma(t)\}$ for all t , then the unwrapping map is the unique inverse of the wrapping map. For manifolds with empty cut loci, unwrapping and wrapping are hence always unique inverses. An example of such a manifold is the set of symmetric positive definite matrices considered in an example in §6.2.

Remark 3.3. The maps in Definition 3.2 either flatten or unflatten curves, and the superscript arrow notation introduced in the definitions is a convenient shorthand notation to make the distinction.

- (i) The unrolling and unwrapping maps are *flattening* maps, indicated by having downarrow ‘ \downarrow ’ within superscript. Downarrow by itself in superscript means unrolling, whereas downarrow accompanied by a curve, say γ , means “unwrapping with respect to γ ”. For example, x_b^\downarrow is the unrolling of curve x into T_bM ; and $x_b^{\downarrow\gamma}$ is the unwrapping of x with respect to γ . Since unwrapping a curve with respect to itself is its unrolling, thus $x_b^{\downarrow x} = x_b^\downarrow$.
- (ii) The rolling and wrapping maps are *unflattening* maps, indicated by uparrow ‘ \uparrow ’ within superscript. Uparrow by itself in superscript means rolling, whereas uparrow accompanied by a curve, say γ , means “wrapping with respect to γ ”. For example, for a curve y_b in T_bM , the curve y_b^\uparrow is its rolling onto M ; and $y_b^{\uparrow\gamma}$ is the wrapping of y_b with respect to γ .

3.2 Rolled Gaussian process model

The maps in the preceding section help define a generative model for random curves on M from a model for curves in \mathbb{R}^d . Let $z(t)$ be a process in \mathbb{R}^d with $E\{z(t)\} = m(t)$, and $y(t) = Uz(t)$ be a process in T_bM with $E\{y(t)\} = \tilde{m}(t) = Um(t)$ for an orthonormal frame $U : \mathbb{R}^d \rightarrow T_bM$. Let the “rolled mean” $\gamma = \tilde{m}^\uparrow$ be the rolling of \tilde{m} onto M , and $x = z^\uparrow\gamma$ be the wrapping of z with respect to γ . In some circumstances, the rolled mean and Fréchet mean of x coincide.

Theorem 3.3 (Rolled mean coinciding with the Fréchet mean). *For every t , the rolled mean, $\gamma(t)$, is the Fréchet mean of $x(t)$ if any of the following conditions are true:*

- (i) *Every point in M has an empty cut locus;*
- (ii) *M is a symmetric manifold, the distribution of $x(t)$ has even symmetry about $\gamma(t)$, and has a unique Fréchet mean that lies outside the cut locus of $\gamma(t)$.*

Theorem 3.3 holds for general processes z with finite mean, not necessarily Gaussian, and is used later when establishing consistency of the estimator of the \tilde{m} in Theorem 4.2. Condition (i) in Theorem 3.3 applies, for example, to non-positively curved manifolds, e.g. d -dimensional hyperbolic space \mathbb{H}^d with the hyperbolic metric and the space $\text{Sym}_{>0}(d)$ of $d \times d$ real symmetric positive definite matrices with several choices of Riemannian metrics; examples of symmetric manifolds relevant to condition (ii) are \mathbb{H}^d and $\text{Sym}_{>0}(d)$, compact manifolds such as \mathbb{S}^2 , rotation matrices, and Lie groups with bi-invariant metrics.

We now define the rolled Gaussian process model. Let $z \sim GP(m, K)$ be a time-indexed Gaussian process in \mathbb{R}^d with mean curve $t \mapsto m(t) = \{m^1(t), \dots, m^d(t)\}^\top \in \mathbb{R}^d$ and covariance $(t, t') \mapsto K(t, t') \in \text{Sym}_{>0}(d)$. The law of z is characterised by the requirement that for every finite r and times t_1, \dots, t_r , the $d \times r$ matrix $Z := \{z(t_1), \dots, z(t_r)\}$ satisfies $\text{vec } Z \sim N_{dr}(\text{vec } M, \Sigma)$, where $M := \{m(t_1), \dots, m(t_r)\} \in \mathbb{R}^{d \times r}$, and Σ is block diagonal with $K(t_i, t_j) \in \text{Sym}_{>0}(d)$ in the (i, j) th block.

Given $b \in M$ and a curve γ on M , let $U = \{u_1, \dots, u_d\}$ be an orthonormal basis on T_bM in its matrix representation. With $\tilde{m}(t) = Um(t) := \sum_{i=1}^d m^i(t)u_i$ and $\tilde{K}(t, t') = UK(t, t')U^\top$, consider the process $y_b(t) := Uz(t)$. On the inner product space $(T_bM, \langle \cdot, \cdot \rangle_b)$ note that $y_b(t)$ is a Gaussian random vector with mean $\tilde{m}(t)$ and covariance determined by the nonnegative linear operator $\tilde{K}(t, t) : T_bM \rightarrow T_bM$; see Appendix 10.1 for details on Gaussians on inner product spaces. As a consequence, $y_b(t) := Uz(t) \sim \mathcal{GP}(\tilde{m}, \tilde{K})$ assuming values in T_bM . We can thus identify a Gaussian process in T_bM with a Gaussian process $z \sim \mathcal{GP}(m, K)$ in \mathbb{R}^d , that when transformed using the wrapping map in Definition 3.2(b) with respect to a curve γ in M , results in a random curve on M whose law is determined by the pair (b, U) and parameters (m, K) .

Definition 3.4 (Rolled Gaussian process). Let $z \sim GP(m, k)$, and choose $b \in M$ and basis U of T_bM . With $\tilde{m}_b = Um$ as a curve in T_bM , let $\gamma := \tilde{m}_b^\uparrow$ be the rolling of \tilde{m} , and let $x = y_b^\uparrow\gamma$ be the wrapping of $y_b := Uz$ with respect to γ . The random curve x on M is a rolled Gaussian process, denoted $x \sim \mathcal{RGP}(m, k; b, U)$.

Of particular note in the definition above is the fact that the Gaussian process z in T_bM is wrapped with respect to the rolling of its mean function \tilde{m} . This is a convenient modelling feature because the curve γ then is not an additional parameter to be estimated, but is instead fully determined by the mean of z . Figure 2 illustrates the construction of the rolled Gaussian process and notation.

The result below identifies the rolled Gaussian process x as the image of a Gaussian vector field along γ under the exponential map, and may be compared with the construction in Mallasto and Feragen [2018]. It uses the notion of a frame along γ detailed in the Appendix 10.2.

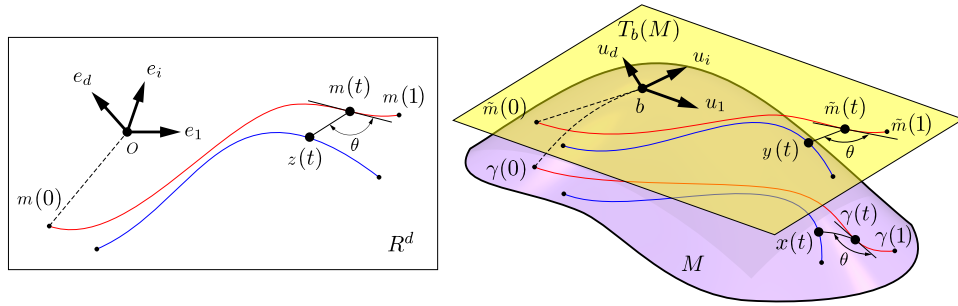


Figure 2: Illustration of how curves defined in \mathbb{R}^d are identified on M , via an intermediate tangent space $T_b M$. Red is the mean curve with respect to which the (un)flattening is performed, and blue is a different curve that deviates from the mean curve. The line segment connecting points between the blue and red curves at arbitrary t , and the corresponding angle denoted θ , indicate distances and angles preserved by the (un)flattening.

Proposition 3.1 (Gaussian vector field along γ). *Let $E^\gamma = \{e_1, \dots, e_d\}$ be a frame along γ . For the pair (b, U) , the random vector field $t \mapsto V^\gamma(t) := E^\gamma(t)y_b(t) = \sum_{i=1}^d y_b^i(t)e_i(t) \in T_{\gamma(t)}M$ along γ is a Gaussian vector field.*

The choice of point $b \in M$ and basis U on its tangent space $T_b M$ is arbitrary. The rolled Gaussian process, however, is equivariant with respect to this choice.

Proposition 3.2 (Equivariance of rolled Gaussian process). *Starting from point $b \in M$ with basis U for $T_b M$, let $x \sim \mathcal{RG}\mathcal{P}(m, K; b, U)$. If one starts instead from $b' \in M$ with basis U' for $T_{b'} M$, then there exists unique m' and K' such that the rolled Gaussian process $x' \sim \mathcal{RG}\mathcal{P}(m', K'; b', U')$ is equal in distribution to x .*

A consequence of this equivariance is that from a practical modelling and computational point of view, the particular choice of b and U is inconsequential.

3.3 A parametric Gaussian process model for random curves on \mathbb{R}^d

A core ingredient of the rolled Gaussian process model in the preceding section is a Gaussian process model, $z \sim \mathcal{GP}(m, K)$, for curves in \mathbb{R}^d to be rolled and wrapped onto M . This model requires specification of the mean, m , and covariance, K , functions. Furthermore, for practical calculations it is helpful to introduce a basis representation for curves, in terms of which m and K can be prescribed and estimated parametrically.

Let $\{\phi_s : [0, 1] \rightarrow \mathbb{R}\}$ be a B-spline basis [De Boor, 2002, Ramsay et al., 2009] of order 4 and knots at the $k - 2$ interior points of a grid of k equally spaced points on $[0, 1]$ with $k \geq \max(4, d)$; then each ϕ_s is a piecewise cubic polynomial with joins at the knots such that any adjacent polynomials' values, and values of first and second derivatives, are matched [De Boor, 2002]. By construction, $\sum_{s=1}^k \phi_s(t) = 1$, for any $t \in [0, 1]$; that is, the constant function is in the span of this basis, a property useful later in Proposition 4.1. Let the mean $m(t) = M_w \phi(t)$, and assume a separable covariance $K(t, t') = \phi(t)^\top V_w \phi(t') U_w$, where $\phi(t) = \{\phi_1(t), \dots, \phi_k(t)\} \in \mathbb{R}^k$ is a vector and $M_w \in \mathbb{R}^{d \times k}$, $U_w \in \text{Sym}_{>0}(d)$ and $V_w \in \text{Sym}_{>0}(k)$ are matrices that parameterise the model, where $\text{Sym}_{>0}(p)$ is the cone of $p \times p$ symmetric positive definite matrices. The convenience of this particular choice is that the curve z can be written

$$z(t) = \sum_{s=1}^k w_s \phi_s(t), \quad (3.7)$$

where $W = (w_1, \dots, w_k) \sim \mathcal{MN}(M_w, U_w, V_w)$, the matrix normal distribution with mean matrix, M_w , row covariance, U_w , and column covariance, V_w . This can be seen by starting from either $z \sim \mathcal{GP}(m, K)$ with the m and K as specified, or from (3.7), and then evaluating at some prescribed inputs t_1, \dots, t_r ; both lead to

$$Z \sim \mathcal{MN}(M_w \Phi, U_w, \Phi^\top V_w \Phi), \quad (3.8)$$

where $\Phi = \{\phi(t_1), \dots, \phi(t_r)\} \in \mathbb{R}^{k \times r}$ and $Z = \{z(t_1), \dots, z(t_r)\} \in \mathbb{R}^{d \times r}$ are matrices.

4 Estimation and inference for curves in discrete time

4.1 Rolling, and the rolled model, in discrete time

In practice, curve data are recorded in discrete time, and a discrete version of the rolled Gaussian process model is accordingly needed. Let t_1, \dots, t_r henceforth be times at which each curve is recorded and stored, with times $t_i = (i-1)/(r-1)$; $i = 1, \dots, r$ assumed equally spaced on $[0, 1]$, and with $r > k$. There is some loss of generality in assuming curves are recorded at common times, and that the observation times are equally spaced, but the former simplifies notation considerably, and both can be easily relaxed. We use upper case for the discrete-time version of the curve denoted in corresponding lower case; for example, $\Gamma := \{\gamma(t_1), \dots, \gamma(t_r)\} \in M^r$ is curve γ in discrete time.

The four maps in §3.1 have natural analogues for discrete curves: the unrolling, Γ_b^\downarrow , of Γ , is the discrete-time curve $\Gamma_b^\downarrow := \{\gamma_b^\downarrow(t_1), \dots, \gamma_b^\downarrow(t_r)\} \in (T_b M)^r$, where γ_b^\downarrow is the unrolling into $T_b M$ of the piecewise geodesic curve that has geodesic segments connecting consecutive points $\gamma(t_i)$ and $\gamma(t_{i+1})$, such that $U^\top \Gamma_b^\downarrow \in \mathbb{R}^{d \times r}$ for a frame $U : \mathbb{R}^d \rightarrow T_b M$. Similarly, $(X)_b^{\downarrow \Gamma}$ with

$$\gamma_b^\downarrow(t_j) + P_{0 \leftarrow 1}^c P_{0 \leftarrow t_j}^\gamma \exp_{\gamma(t_j)}^{-1} \{x(t_j)\}$$

as the j th component is the unwrapping of a discrete-time curve $X \in M^r$ with respect to the same piecewise geodesic γ such that $U^\top (X)_b^{\downarrow \Gamma} \in \mathbb{R}^{d \times r}$. The unflattening maps, rolling and wrapping, for discrete curves follow in a similar way to these flattening ones; see Appendix 10.3.

For the discrete-time version of model $x \sim \mathcal{RG}\mathcal{P}(m, K; b, U)$ under the parametric specification of m and K from §3.3, we write

$$X \sim \mathcal{RMN}(M_w, U_w, V_w; b, U). \quad (4.1)$$

A random draw from (4.1) is simulated by drawing random Z from (3.8) then, with respect to base point b and basis U , wrapping Z with respect to the rolling of the mean $M = M_w \Phi$. We spell out these steps in §5 in practical embedding coordinates that are convenient for numerical computations. Section §6.1 shows a concrete example in the special case with manifold $M = \mathbb{S}^2$, the unit 2-sphere in \mathbb{R}^3 , of the model (4.1) being prescribed and simulated from; the simulations are shown in Fig. 3.

Prior to considering estimation in the next section, it is helpful first to define the following *unwrapping coordinates* for the discretised curves.

Definition 4.1 (Unwrapping coordinates). Let $\Gamma = \{\gamma(t_1), \dots, \gamma(t_r)\}$ and $X = \{x(t_1), \dots, x(t_r)\}$ respectively be discrete-time versions of arbitrary curves γ and x in M . Fix $b \in M$ and frame U for $T_b M$. When x and γ are outside the cut loci of each other, and b is outside the cut locus of $\gamma(0)$, the unwrapping coordinates of X are defined by the map

$$(X, \Gamma) \mapsto H(X, \Gamma) := U^\top (X)_b^{\downarrow \Gamma}. \quad (4.2)$$

This definition reverses the steps described for defining X in (4.1), in which the X were defined in terms of Z . Indeed, if the conditions of Remark 3.2 hold, and if $\Gamma = (UM_w\Phi)_b^\uparrow$ is the rolled path in the generative model, then (4.2) implies that $(X_i)_b^{\downarrow\Gamma} = Y_i$, and, due to (3.8),

$$H(X_i; \Gamma) = Z_i \sim \mathcal{MN}(M_w\Phi, U_w, \Phi^\top V_w\Phi), \quad (4.3)$$

that is, the underlying $\{Z_i\}$ in the generative model are exactly recovered. The foregoing steps rely on the b and U in (4.2) being the same b and U in the definition of $\{X_i \sim \mathcal{RMN}(M_w, U_w, V_w; b, U)\}$ in that generative model; however, the following proposition establishes that using alternative b' and U' leads to unwrapping coordinates, and hence model parameters, that differ only equivariantly. Choose $b' \in M$ and basis U' for $T_{b'}M$, and let c' be a geodesic from b' to $\gamma(0)$.

Proposition 4.1 (Equivariance with respect to b, U). *Let $H'(X_i; \Gamma) = U'^\top (X_i)_{b'}^{\downarrow\Gamma}$, let $H(X_i; \Gamma) \sim \mathcal{MN}(M_w\Phi, U_w, \Phi^\top V_w\Phi)$, and suppose that the constant function is in the span of the basis, Φ . Then there exists $a \in \mathbb{R}^d$ and a linear isometry $A : \mathbb{R}^d \rightarrow \mathbb{R}^d$ such that $H'(X_i; \Gamma) = a1_r^\top + AH(X_i; \Gamma) \sim \mathcal{MN}(M'_w\Phi, U'_w, \Phi^\top V_w\Phi)$, where $M'_w = a1_k^\top + AM_w$ and $U'_w = AU_wA^\top$.*

Under matrix representations of the parallel transport maps, the operator A is an orthogonal matrix. This Proposition is an analogue of Proposition 3.2, specialised to the model §3.3 and to discrete time; it establishes the practical sense in which the choice of b, U are inconsequential.

4.2 Estimation

First we consider the problem in which we are given $\{Z_i\}_{i=1, \dots, n}$, each Z_i assumed to be an independent realisation of (3.8), and the goal is to estimate the parameters M_w, U_w , and V_w . For this, it is helpful to define the right-inverse, $\Phi^- = \Phi^\top(\Phi\Phi^\top)^{-1}$, of Φ such that $\Phi\Phi^- = I_k$, the k -dimensional identity matrix; this right-inverse is unique since the basis $\{\phi_s\}$ defined above is such that Φ has full row rank, k . Then $\{W_i = Z_i\Phi^-\}_{i=1, \dots, n}$ are independent realisations from the distribution $\mathcal{MN}(M_w, U_w, V_w)$, for which the logarithm of the likelihood function, omitting the constant term not dependent on the parameters, is [Duttilleul, 1999]

$$\ell = -\frac{mn}{2} \log(|U_w|) - \frac{kn}{2} \log(|V_w|) - \frac{1}{2} \sum_{i=1}^n \text{tr} \{U_w^{-1}(W_i - M_w)V_w^{-1}(W_i - M_w)^\top\}. \quad (4.4)$$

The maximum likelihood estimator of the mean matrix is $\hat{M}_w = n^{-1} \sum_{i=1}^n W_i$; this is also the least-squares estimator, that is, the minimiser of $M_w \mapsto \sum_{i=1}^n \text{tr} \{(W_i - M_w)(W_i - M_w)^\top\}$. Maximum likelihood estimators \hat{U}_w, \hat{V}_w satisfy the pair of equations

$$\hat{U}_w = \frac{1}{nk} \sum_{i=1}^n (W_i - \hat{M}_w)\hat{V}_w^{-1}(W_i - \hat{M}_w)^\top; \quad \hat{V}_w = \frac{1}{nd} \sum_{i=1}^n (W_i - \hat{M}_w)^\top \hat{U}_w^{-1}(W_i - \hat{M}_w), \quad (4.5)$$

which can be evaluated iteratively until convergence [Duttilleul, 1999].

Now consider the more challenging problem where the data are curves on M . For a sample of discrete-time curves $\{X_i\}_{i=1, \dots, n}$, each $X_i \sim \mathcal{RMN}(M_w, U_w, V_w; b, U)$ independently for a fixed point $b \in M$ and basis U of T_bM , the goal is to estimate parameters M_w, U_w , and V_w . Parameters M_w, V_w, U_w may be estimated by maximising a likelihood written using (4.4) for the mean and covariance parameters in (4.3); moreover, $H(\Gamma; \Gamma) = M_w\Phi$.

Of course, Γ , is not known *a priori*; under the generative model it depends on M_w , which is to

be estimated. Two candidate estimators are:

$$\hat{M}_w^{\text{LS}} = \underset{M_w}{\operatorname{argmin}} \sum_{i=1}^n \operatorname{tr} \left[\{H(X_i; \Gamma)\Phi^- - M_w\} \{H(X_i; \Gamma)\Phi^- - M_w\}^\top \right], \quad (4.6)$$

$$\hat{M}_w^{\text{MLE}} = \underset{M_w}{\operatorname{argmin}} \sum_{i=1}^n \operatorname{tr} \left[\hat{U}_w^{-1} \{H(X_i; \Gamma)\Phi^- - M_w\} \hat{V}_w^{-1} \{H(X_i; \Gamma)\Phi^- - M_w\}^\top \right], \quad (4.7)$$

in which $\Gamma = \Gamma(M_w)$, that is, in (4.6) and (4.7), since Γ is determined by M_w , it is implicitly being estimated jointly with M_w . The estimators \hat{M}_w^{LS} and \hat{M}_w^{MLE} require numerical optimisation; in computations we have used the Broyden–Fletcher–Goldfarb–Shannon algorithm as implemented in the `optim` function in R [R Core Team, 2023]. Estimators of U_w and V_w are

$$\hat{U}_w = \frac{1}{nk} \sum_{i=1}^n \left\{ H(X_i; \Gamma(\hat{M}_w))\Phi^- - \hat{M}_w \right\} \hat{V}_w^{-1} \left\{ H(X_i; \Gamma(\hat{M}_w))\Phi^- - \hat{M}_w \right\}^\top, \quad (4.8)$$

$$\hat{V}_w = \frac{1}{nd} \sum_{i=1}^n \left\{ H(X_i; \Gamma(\hat{M}_w))\Phi^- - \hat{M}_w \right\}^\top \hat{U}_w^{-1} \left\{ H(X_i; \Gamma(\hat{M}_w))\Phi^- - \hat{M}_w \right\}, \quad (4.9)$$

related to (4.5), in which $\hat{M}_w \in \{\hat{M}_w^{\text{LS}}, \hat{M}_w^{\text{MLE}}\}$. If \hat{M}_w is taken to be \hat{M}_w^{LS} , then it can be evaluated once at the outset, followed by iterative evaluations of (4.8) and (4.9). If \hat{M}_w is taken to be \hat{M}_w^{MLE} then, owing to its dependence on \hat{U}_w and \hat{V}_w , it becomes necessary to evaluate (4.7), (4.8) and (4.9) iteratively. One reason that \hat{M}_w^{MLE} might be preferred in spite of this extra computational cost is that in the case where the manifold M has non-positive sectional curvatures then \hat{M}_w^{MLE} together with \hat{U}_w \hat{V}_w in (4.8, 4.9) are asymptotically, for large n , the maximum likelihood estimators, and are exactly so when Γ is the data-generating curve.

Another estimator of Γ is based on the discretization of the sample Fréchet mean curve, when it exists, which can then be used to estimate M_w . The discrete version of the sample Fréchet mean, defined in (2.3), is $\hat{\Gamma}_{\text{Fre}} = \{\hat{\gamma}_{\text{Fre}}(t_1), \dots, \hat{\gamma}_{\text{Fre}}(t_n)\}$. An estimator of M_w based on the unwrapped coordinates with respect to $\hat{\Gamma}_{\text{Fre}}$ is

$$\hat{M}_w^{\text{Fre}} = \underset{M_w}{\operatorname{argmin}} \sum_{i=1}^n \operatorname{tr} \left[\left\{ H(X_i; \hat{\Gamma}_{\text{Fre}})\Phi^- - M_w \right\} \left\{ H(X_i; \hat{\Gamma}_{\text{Fre}})\Phi^- - M_w \right\}^\top \right]. \quad (4.10)$$

In practice, especially for data on M with small variability for each t , we have found barely any appreciable difference between estimators \hat{M}_w^{Fre} , \hat{M}_w^{LS} , \hat{M}_w^{MLE} . However, \hat{M}_w^{Fre} has practical advantages in having a closed-form expression in terms of the sample Fréchet mean curve, $\hat{\Gamma}_{\text{Fre}}$, and having a natural interpretation as being expressible via the unrolling of $\hat{\Gamma}_{\text{Fre}}$ onto $T_b M$.

Proposition 4.2 (Estimator \hat{M}_w^{Fre} via unrolling of the sample Fréchet mean). *Assume that the sample Fréchet mean curve in (2.3) exists and is unique. Then,*

$$\hat{M}_w^{\text{Fre}} = H(\hat{\Gamma}_{\text{Fre}}; \hat{\Gamma}_{\text{Fre}})\Phi^-.$$

Under the conditions of Theorem 3.3 which relates the Fréchet mean and the rolled mean, we prove that the estimator \hat{M}_w^{Fre} is consistent for M_w whenever the sample Fréchet mean curve, $\hat{\gamma}_{\text{Fre}}$ consistently estimates γ_{Fre} , under rolled Gaussian process model $x \sim \mathcal{RG}\mathcal{P}(m, K; b, U)$ in a topology strong enough to ensure convergence of the parallel transport maps.

Theorem 4.2 (Consistency of estimator \hat{M}_w^{Fre}). *Assume that the population Fréchet mean curve γ_{Fre} in (2.2) exists and is unique. Suppose $\hat{\gamma}_{\text{Fre}}$ converges in probability, as $n \rightarrow \infty$, in the C^1 topology to the population mean curve γ under the rolled Gaussian process model. Then, under any of the conditions in Theorem 3.3, as $n \rightarrow \infty$, \hat{M}_w^{Fre} converges in probability to M_w .*

Remark 4.1. C^1 convergence of curves in Theorem 4.2 is stronger than what is necessary to establish consistency of the estimator \hat{M}_w^{Fre} , since only necessary is convergence of parallel transport maps along their piecewise geodesic approximations at the finite times t_1, \dots, t_m .

4.3 A two-sample test for equality of mean curves

The flattening operation using the unrolling and unwrapping maps enable development of inferential tools for samples of curves on M . We briefly discuss how this can be done for a two-sample test of equality of means of two samples $\{X_1^{(1)}, \dots, X_{n_1}^{(1)}\}$ and $\{X_1^{(2)}, \dots, X_{n_2}^{(2)}\}$ of curves on M , which we anticipate will be relevant in many applications. A resampling-based test for equality of mean curves, using a test statistic analogous to the Hotelling T^2 statistic in classical multivariate setting, is as follows. Suppose that

$$X_i^{(g)} \sim \mathcal{RMN}(M_w^{(g)}, U_w, V_w; b, U),$$

in which for $g = 1, 2$ the mean parameters are possibly different, but the covariance parameters are assumed common. In this context, the hypothesis to test is $H_0 : M_w^{(1)} = M_w^{(2)}$ versus the alternative $H_1 : M_w^{(1)} \neq M_w^{(2)}$. From §4.2, given estimates $\hat{M}_w^{(g)}, \hat{U}_w^{(g)}, \hat{V}_w^{(g)}$ for each sample, the analogue of the Hotelling T^2 statistic is

$$J = \text{tr} \left\{ \hat{V}_w^{-1} (\hat{M}_w^{(1)} - \hat{M}_w^{(2)})^\top \hat{U}_w^{-1} (\hat{M}_w^{(1)} - \hat{M}_w^{(2)}) \right\}, \quad (4.11)$$

in which $\hat{U}_w = \{(n_1 - 1)\hat{U}_w^{(1)} + (n_2 - 1)\hat{U}_w^{(2)}\}/(n_1 + n_2 - 2)$ is a pooled estimate of U_w , and V_w is defined similarly. The null hypothesis is rejected for suitably large J with respect to its null distribution, which is accessed by resampling. For a permutation test, the procedure is: pool the two samples as $\{X_1^{(1)}, \dots, X_{n_1}^{(1)}, X_1^{(2)}, \dots, X_{n_2}^{(2)}\}$ then partition randomly to create resampled data, $\{X_1^{(1)*}, \dots, X_{n_1}^{(1)*}\}$ and $\{X_1^{(2)*}, \dots, X_{n_2}^{(2)*}\}$, say, from which to compute the statistic (4.11). Doing this a large number, say R , times gives resampled statistics J_1^*, \dots, J_R^* that can be treated as a sample from the null distribution of J . The p -value can be computed as $p = \{1 + \sum_r \mathbb{I}(J_r^* > J)\}/(1 + R)$, where \mathbb{I} is the indicator function. The step of randomly partitioning the pooled data can be replaced by sampling with replacement from the pooled data, to give a bootstrap test. Results later in §7 use the permutation version described above.

5 Practical calculations in embedded coordinates

For computations, it is convenient to regard M as a d -dimensional embedded Riemannian submanifold of \mathbb{R}^q , for $d < q$, with the induced metric from \mathbb{R}^q ; when $d = q$, M is an open submanifold of \mathbb{R}^q , and specific Riemannian metrics may be chosen. Given the global coordinates of \mathbb{R}^q , a point p in M and vector in $T_p M$ are both represented as vectors in \mathbb{R}^q . With such a choice of coordinates, it is natural to identify the tangent space $T_p M$ with the d -dimensional affine subspace $\{p + T_p M\}$ in \mathbb{R}^q . Thus, in coordinates of \mathbb{R}^q , the unrolling γ_b^\downarrow of γ satisfies (3.4) subject to initial condition $\gamma_b^\downarrow(0) = b + \exp_b^{-1}\{\gamma(0)\}$, with solution

$$\gamma_b^\downarrow(t) = b + \exp_b^{-1}\{\gamma(0)\} + P_{0 \leftarrow 1}^c \{\gamma^\downarrow(t) - \gamma^\downarrow(0)\}; \quad (5.1)$$

rolling γ_b^\uparrow is defined as previously as the unique inverse of unrolling, and the unwrapping and wrapping maps are as defined before in (3.5-3.6) with elements of M or $T_b M$ being vectors in \mathbb{R}^q , and each parallel transport being a matrix, $\mathbb{R}^{q \times q}$. For the rolled Gaussian process $x \sim \mathcal{RGP}(m, K; b, U)$ in embedded coordinates, basis $U = (u_1, \dots, u_d) \in \mathbb{R}^{q \times d}$ is a matrix with d

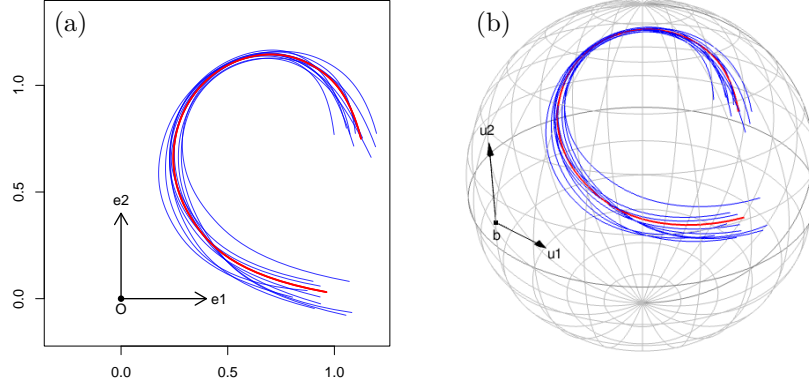


Figure 3: (a) Curves from the model in \mathbb{R}^2 described in §6.1. (b) Corresponding rolled and wrapped curves on \mathbb{S}^2 .

orthonormal columns, and the Gaussian process $z \sim \mathcal{GP}(m, K)$ is such that $z(t) = \sum_{i=1}^d e_i z(t)$ where $\{e_i\}$ is the standard basis for \mathbb{R}^d ; then for $\tilde{m}_b : \tilde{m}_b(t) = b + \sum_{i=1}^d u_i m(t)$ and $y : y(t) = b + \sum_{i=1}^d u_i z(t)$, $\gamma = \tilde{m}_b^\uparrow$ is the rolled mean, and finally $x = y_b^\uparrow^\gamma$.

Recall that the discrete-time model (4.1) for curves on M is based upon rolling and wrapping curves from the underlying model (3.8) for curves on \mathbb{R}^d . Let $\tilde{M} = b1_r^\top + UM_w\Phi$ be the mean curve in (3.8) identified as a curve in T_bM , and $\Gamma = (\tilde{M})_b^\uparrow$ be its rolling onto M ; for Z a random curve from (3.8), $Y = b1_r^\top + UZ$ is the corresponding curve in T_bM , and $X = Y_b^\uparrow^\Gamma$ its wrapping with respect to Γ onto M .

For a curve X on M , the curve's unwrapping coordinates (4.2), with the unwrapping being with respect to the curve Γ , are

$$H(X_i; \Gamma) = U^\top \left\{ (X_i)_b^\uparrow^\Gamma - b1_r^\top \right\}. \quad (5.2)$$

6 Numerical examples

6.1 A prescribed model for heteroscedastic curves on \mathbb{S}^2

Here we give an example for $M = \mathbb{S}^2$, of the steps described in the preceding section to simulate from (4.1) for curves on \mathbb{S}^2 : first define a model (3.8) in \mathbb{R}^2 , with prescribed parameters M_w, U_w, V_w , simulate for the model in \mathbb{R}^2 then roll and wrap to produce curves \mathbb{S}^2 that are samples from (4.1). Let s_1, \dots, s_k be an equally spaced sequence of points spanning $[0, 1]$, $M_w \in \mathbb{R}^{2 \times k}$ be the matrix with i th column equal to $3/4 \cdot [(1, 1) + (1/2 + s_i^2/2) \cdot \{\cos(5s_i), \sin(5s_i)\}]^\top$, and $k = 10$. The mean curve, $m(t) = M_w\phi(t)$, evaluated discretely as $M_w\Phi$ at $r = 100$ values of t equally spaced on $[0, 1]$, is shown as the red line in Fig. 3(a). To prescribe the covariance parameters, let $U_w = I_2$, and let V_w be the matrix with (i, j) th element equal to $a_i a_j \rho^{|i-j|}$, with $a_i = 1 + 3/4 \cdot \cos(2\pi i/k)$ and $\rho = 0.9$. This prescription produces curves in \mathbb{R}^2 with smooth variation and some moderate heteroscedasticity. A random curve from this model is $z_i(t) = W_i\phi(t)$, with $W_i \sim \mathcal{MN}(M_w, U_w, V_w)$, evaluated numerically as $Z_i = W_i\Phi$. Fig. 3(a) shows a sample of $n = 10$ curves from this model.

To roll the model onto \mathbb{S}^2 , using the embedding coordinates of \mathbb{R}^3 , we fix $b = (51)^{-1}(-5, -5, 1)^\top \in \mathbb{S}^2$, an arbitrary choice, and fix $U \in \mathbb{R}^{3 \times 2}$, the basis matrix for $T_b\mathbb{S}^2$, by taking its columns to be the left singular vectors of $(I_3 - bb^\top)$, excluding the column corresponding to the zero singular

Estimator	Metric	Sample Size, n				
		10	25	50	100	500
\hat{M}_w	$\text{tr}\{U_w^{-1}(\hat{M}_w - M_w)V_w^{-1}(\hat{M}_w - M_w)^\top\}$	2.19	0.46	0.30	0.14	0.10
\hat{U}_w	$d(\hat{U}_w, U_w)$	0.47	0.27	0.19	0.15	0.06
\hat{V}_w	$d(\hat{V}_w, V_w)$	1.16	0.72	0.55	0.32	0.15

Table 1: Results of numerical investigation into convergence of parameter estimates with increasing n , for the $\text{Sym}_{>0}(2)$ model in §6.2

value. The rolled mean is $\Gamma = (b\mathbf{1}_r^\top + UM_w\Phi)_b^\uparrow$, and the random curves wrapped with respect to this rolled mean are $X_i = (b\mathbf{1}_r^\top + UZ_i)_b^\uparrow \sim \mathcal{RMN}(M_w, U_w, V_w; b, U)$. Figure 3(b) shows the curves on M ; red is the rolled mean, Γ , and blue are the wrapped curves, $\{X_i\}$.

6.2 Curves on $\text{Sym}_{>0}(2)$

We equip the three-dimensional manifold $\text{Sym}_{>0}(2)$ with the affine-invariant metric, $d(\cdot, \cdot)$, which makes it negatively curved [e.g. Pennec et al., 2019, Chapter 3]; see 10.5 for definition of $d(\cdot, \cdot)$. The global coordinates of \mathbb{R}^3 is used to define a model with parameters M_w, U_w, V_w and roll onto $\text{Sym}_{>0}(2)$, then from simulated data try to infer the parameters. With s_1, \dots, s_k an equally spaced sequence of points spanning $[0, 1]$ and $k = 5$, let $M_w \in \mathbb{R}^{3 \times k}$ be the matrix with i th column equal to $3/4 \cdot [(1/5) \cdot \{\cos(5s_i), \sin(5s_i), s_i\}]^\top$, $U_w = I_3$, and V_w be the matrix with (i, j) th element equal to $10^{-3}a_i a_j \rho^{|i-j|}$, with a_i, ρ as in §6.1. We take the tangent point $b = I_2$ and basis for tangent space $U = I_3$, then simulate data $\{X_i\}$ as in §6.1. Table 1 shows numerical results from simulating the data then fitting the model to the simulated data, to investigate convergence of estimators $\hat{M}_w = \hat{M}_w^{\text{Fre}}$ from (4.10) and \hat{U}_w and \hat{V}_w from (4.8) and (4.9) to their data-generating values. Results in the table show each estimator, with respect to the indicated metric, getting closer to towards its population counterpart as the sample size, n , increases; a Mahalaonobis-type metric is used for \hat{M}_w and $d(\cdot, \cdot)$ is used for \hat{U}_w and \hat{V}_w .

7 Application: orientation of end-effector of a robot arm, curves on $SO(3)$

The data are orientations of the end-effector of a Franka robot arm as it was guided $n = 60$ times by the third author to perform a task to deposit the contents of a dustpan into a bin. The orientation can be represented by an element of $SO(3)$, the set of 3-by-3 orthogonal matrices with unit determinant, that describes its rotation from an initial reference orientation. An element of $SO(3)$ may be parameterised as an unsigned unit quaternion, and $SO(3)$ is hence identified with \mathbb{S}^3 modulo the antipodal map [Prentice, 1986]. Fixing the sign of each data point (e.g. to positive) then identifies $SO(3)$ with a hemisphere of \mathbb{S}^3 , which is our manifold M equipped with the induced geometry of \mathbb{S}^3 , whose geometry is inherited from \mathbb{R}^4 .

The curves, X_i , are recorded at $r = 100$ time points. We choose basis dimension $k = 10$, and set $b = e_1$ and $U = (e_2, e_3, e_4)$, where $\{e_i\}$ is the standard basis for \mathbb{R}^4 . We compute the estimated mean curve $\hat{\Gamma} = (b\mathbf{1}_r^\top + U\hat{M}_w\Phi)_b^\uparrow$, with \hat{M}_w estimated as in (4.6). Then the unwrapping coordinates, $H_i = H(X_i; \hat{\Gamma})$ for $H(\cdot; \cdot)$ in (4.2), are curves in \mathbb{R}^3 ; these are shown as blue curves in Fig. 4(a), together with corresponding unrolled mean, $H(\hat{\Gamma}; \hat{\Gamma})$, plotted in red. The curves have a common starting point at $t = 0$, shown near the top-left in this plot; for small t the variability is small, but then at larger t there is much larger variability, especially following a kink point that corresponds to the dustpan being turned to empty its contents. We further estimate the covariance

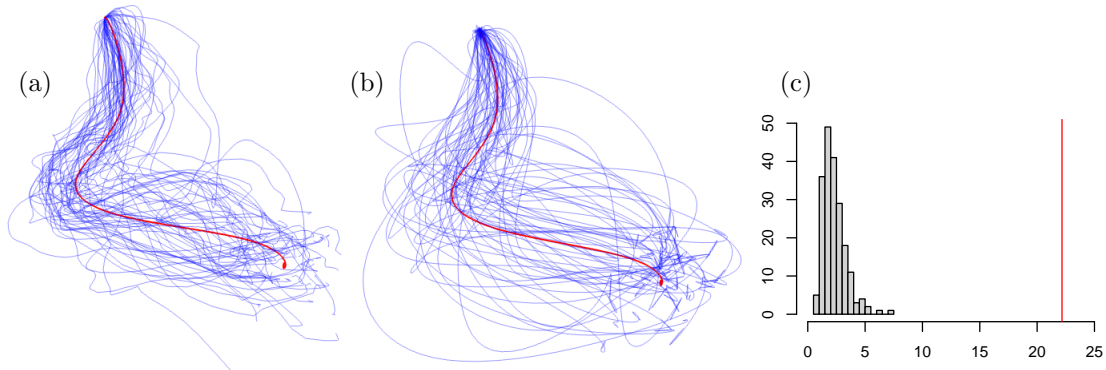


Figure 4: For robot $\text{SO}(3)$ curves described in §7: (a) unwrapped data, blue, and unrolled fitted mean, red; (b) simulations from the fitted Gaussian process model; (c) bootstrap null distribution for test described in text.

matrices U_w and V_w in (4.1) using (4.8, 4.9). As a visual appraisal of the fitted model, Fig. 4(b) shows $n = 60$ realisations from $\mathcal{RMN}(M_w, \hat{U}_w, \hat{V}_w; b, U)$, using the same unwrapping coordinates and projection as in Fig. 4(a). These simulated curves are smoother than the real data, which is a consequence of the basis used, but they have similar heteroscedastic variation.

A feature of these data is that they were collected over two sessions, so the data are in fact two samples each of $n^{(g)} = 30$ curves, where $g \in \{1, 2\}$ indexes the sample. An interesting statistical question is whether the two samples have different statistical characteristics. We perform the test described in §4.3 to test the null hypothesis that two samples arise from populations with equal mean curve. Figure 4(c) shows a histogram of values of test statistic J in (4.11) simulated under the null hypothesis of equal means, using the permutation procedure described in §4.3 with $R = 200$ resamples, and the red line shows the observed value of the statistic $J = 22.17$ computed from the data. This observed value is extreme compared with the null distribution, providing conclusive evidence against the null hypothesis of equal means.

8 Discussion

The rolling approach presented here extends beyond the Gaussian process setting. Future work will explore rolling and wrapping of other processes on \mathbb{R}^d to develop other useful new models on manifolds M .

For our examples, we leveraged closed-form expressions for exponential, inverse exponential, and parallel transport maps when computing with the four maps in §3.1. On manifolds lacking these closed-form expressions, approximations via retractions and their inverses offer practical alternatives [Absil et al., 2009].

Within the Gaussian process setting of this paper, we have specialised to a particular parameterization of the mean and covariance, and assumed common and equispace observation times; these provide modelling and computational convenience but are straightforward to relax. A further generalization is to incorporate a model of nuisance variation in the time variable via warping. This would accommodate the possibility of time registration of observed curves, often valuable in analogous Euclidean settings [Zhang et al., 2018, Su et al., 2014]. However, for rolled models, warping combined with rolling raises challenges for computation and inference that remain to be resolved. The foregoing points present exciting opportunities to exploit the strategy of rolling in wider settings involving data on manifolds.

9 Acknowledgements

We thank Huling Le for helpful discussions. SP acknowledges support from a grant from the Engineering and Physical Sciences Research Council (EPSRC EP/T003928/1). KB acknowledges support from grants from the Engineering and Physical Sciences Research Council (EPSRC EP/X022617/1), National Science Foundation (NSF 2015374), and the National Institutes of Health (NIH R37-CA21495).

10 Appendix

10.1 Gaussian distribution on inner product spaces

We briefly review the concepts required for our purposes and refer to Eaton [1983] for more details. Let $(X, \langle \cdot, \cdot \rangle_X)$ be a d -dimensional vector space. With respect to a probability space $(\Omega, \mathcal{F}, \mathbb{P})$ if a random vector Z in X is such that $E(\langle x, Z \rangle_X) < \infty$ for every $x \in X$, there exists a unique vector $\mu \in X$, known as the *mean* of Z , such that $E(\langle x, Z \rangle_X) = \langle \mu, Z \rangle_X$; we can employ the notation $\mu = EZ$.

In similar fashion, with Cov as the usual covariance between real-valued random variables, if $E(\langle x, Z \rangle_X^2) < \infty$ for every $x \in X$, the unique non-negative linear operator $\Sigma : X \rightarrow X$ that satisfies

$$\text{Cov}(\langle x, Z \rangle_X, \langle y, Z \rangle_X) = \langle x, \Sigma y \rangle_X, \quad \forall x, y \in X,$$

is referred to as the *covariance* of Z . Let $(Y, \langle \cdot, \cdot \rangle_Y)$ be another d -dimensional inner product space, and $\mathcal{L}(X, Y)$ be the space of bounded linear operators from X to Y . Given a random vector Z in X with mean μ and covariance Σ , the random vector CZ for $C \in \mathcal{L}(X, Y)$ has mean $C\mu$ and $C\Sigma C^\top$, where $C^\top \in \mathcal{L}(Y, X)$ is the unique adjoint of C which satisfies $\langle b, Ca \rangle_Y = \langle C^\top b, a \rangle_X$ for all $a \in X$ and $b \in Y$.

The following provides a basis-free definition of a Gaussian distribution on an inner product space.

Definition 10.1. A random vector $Z \in (X, \langle \cdot, \cdot \rangle_X)$ has a Gaussian distribution with mean μ and covariance Σ if for every $x \in X$ the real-valued random variable $\langle x, Z \rangle$ has a Gaussian distribution on \mathbb{R} with mean $\langle x, \mu \rangle_X$ and variance $\langle x, \Sigma x \rangle_X$.

With respect to $(\Omega, \mathcal{F}, \mathbb{P})$ suppose X_1 and X_2 are two random vectors on $(X_1, \langle \cdot, \cdot \rangle_{X_1})$ and $(X_2, \langle \cdot, \cdot \rangle_{X_2})$, respectively, with covariances Σ_1 and Σ_2 . The random vector (X_1, X_2) then assumes values in the direct sum space $X_1 \oplus X_2$ equipped with the inner product $\langle \cdot, \cdot \rangle_{X_1} + \langle \cdot, \cdot \rangle_{X_2}$. A well-defined positive semidefinite bilinear map $(x_1, x_2) \mapsto \text{Cov}(\langle x_1, X_1 \rangle_{X_1}, \langle x_2, X_2 \rangle_{X_2})$ ensures the existence of a unique operator $\Sigma_{12} \in \mathcal{L}(X_1, X_2)$. Then, the linear operator $\Sigma \in \mathcal{L}(X_1 \oplus X_2, X_1 \oplus X_2)$ defined as $\Sigma(x_1, x_2) = (\Sigma_{11}x_1 + \Sigma_{12}x_2, \Sigma_{12}^\top x_1, \Sigma_{22}x_2)$, is known as the covariance of the random vector (X_1, X_2) in $X_1 \oplus X_2$. The above definition extends easily to random vectors (X_1, \dots, X_m) with values in $X_1 \oplus \dots \oplus X_m$.

10.2 Orthonormal frame along a curve γ

Denote by $\mathfrak{X}(\gamma)$ the set of vector fields along a curve $\gamma : [0, 1] \rightarrow M$. The intrinsic description requires a curve $\gamma : [0, 1] \rightarrow M$ and an orthonormal frame $E^\gamma = (e_1, \dots, e_d)$ with $e_i \in \mathfrak{X}(\gamma)$, $i = 1, \dots, d$ such that $E^\gamma(\gamma(t)) = (e_1(\gamma(t)), \dots, e_d(\gamma(t)))$ is an orthonormal basis of $T_{\gamma(t)}M$ for every t . Simplify notation using $E^\gamma(t) = (e_1(t), \dots, e_d(t))$ to denote the frame, and note that E^γ is obtained by choosing a basis (v_1, \dots, v_d) for $T_{\gamma(0)}M$, and setting $E^\gamma(t) := (P_{t \leftarrow 0}^\gamma v_1, \dots, P_{t \leftarrow 0}^\gamma v_d)$ to be a parallel frame with $e_i(t) = P_{t \leftarrow 0}^\gamma v_i$. Then every vector field $V \in \mathfrak{X}(\gamma)$ may be expressed as $V(t) = \sum_{i=1}^d V^i(t)e_i(t)$, where $t \mapsto V^i(t) \in \mathbb{R}$ are component functions.

If instead we start with an orthonormal basis $U = (u_1, \dots, u_d)$ of the tangent space T_bM of a point $b \in M$, the orthonormal frame E^γ is obtained by first choosing $v_i = P_{1 \leftarrow 0}^c u_i$, where $P_{t \leftarrow s}^c : T_{c(s)}M \rightarrow T_{c(t)}M$ is the parallel transport along the (unique) geodesic $c : [0, 1] \rightarrow M$ with $c(0) = b$ and $c(1) = \gamma(0)$, so that

$$E^\gamma(t) = (P_{t \leftarrow 0}^\gamma P_{1 \leftarrow 0}^c u_1, \dots, P_{t \leftarrow 0}^\gamma P_{1 \leftarrow 0}^c u_d), \quad t \in [0, 1].$$

In other words, the vector fields $e_i := P_{t \leftarrow 0}^\gamma P_{1 \leftarrow 0}^c u_i, i = 1, \dots, d$ that constitute E^γ are parallel vector fields in $\mathfrak{X}(\gamma)$ along γ determined by U . Note that $E^\gamma(0)$ depends on the curve γ only through $\gamma(0)$ via the geodesic c connecting b to $\gamma(0)$. Thus for each t , $E^\gamma(t) : T_bM \rightarrow T_{\gamma(t)}M$ is a linear isomorphism engendered by its definition using parallel transport maps on the basis U of T_bM .

10.3 Computations with discrete representations of curves

Numerical implementation necessarily entails discrete representations of continuous curves; for example, the base curve $t \rightarrow \gamma(t)$ that determines rolling is stored as $\Gamma = \{\gamma(t_1), \dots, \gamma(t_m)\}$. This discrete representation, Γ , can be regarded as a piecewise geodesic approximation of γ that coincides with γ at t_1, \dots, t_m and that can be made arbitrarily accurate by making the time discretization arbitrarily fine. Define $\tilde{\gamma}$ as a piecewise geodesic curve with geodesic segments connecting consecutive elements of Γ , to approximate γ in computations. Then, for example, parallel transport along the discretized curve, Γ , is

$$P_{t \leftarrow t_0}^{\tilde{\gamma}} = P_{t \leftarrow t_j}^{\tilde{\gamma}} \cdots P_{t_2 \leftarrow t_1}^{\tilde{\gamma}} P_{t_1 \leftarrow t_0}^{\tilde{\gamma}},$$

here for t satisfying $t_j \leq t \leq t_{j+1}$; in other words, the parallel transport is a composition of parallel transports each along a geodesic, enabling simple computation. To compute the discretized unrolling, $\Gamma^\downarrow = \{\gamma^\downarrow(t_1), \dots, \gamma^\downarrow(t_m)\}$, of Γ , from (3.1) and with $\tilde{\gamma}$ replacing γ ,

$$\begin{aligned} \gamma^\downarrow(t) &= \gamma(t_0) + \left(\int_{t_0}^{t_1} + \cdots + \int_{t_j}^t \right) P_{t_0 \leftarrow s}^{\tilde{\gamma}} \dot{\tilde{\gamma}}(s) ds \\ &= \gamma^\downarrow(t_j) + \int_{t_j}^t P_{t_0 \leftarrow t_j}^{\tilde{\gamma}} P_{t_j \leftarrow s}^{\tilde{\gamma}} \dot{\tilde{\gamma}}(s) ds = \gamma^\downarrow(t_j) + P_{t_0 \leftarrow t_j}^{\tilde{\gamma}} \exp_{\gamma(t_j)}^{-1} \tilde{\gamma}(t), \end{aligned} \quad (10.1)$$

using recursion, and using that along the geodesic segment between $\tilde{\gamma}(t_j)$ and $\tilde{\gamma}(t)$, $\int_{t_j}^t P_{t_j \leftarrow s}^{\tilde{\gamma}} \dot{\tilde{\gamma}}(s) ds = t \dot{\tilde{\gamma}}(t_j) = \exp_{\gamma(t_j)}^{-1} \tilde{\gamma}(t)$. Hence, via equation (10.1), $\Gamma^\downarrow = \{\gamma^\downarrow(t_1), \dots, \gamma^\downarrow(t_m)\}$ can be determined from $\Gamma = \{\gamma(t_1), \dots, \gamma(t_m)\}$. Similarly, via the rearrangement of (10.1) as

$$\gamma(t) = \exp_{\gamma(t_j)} \left[P_{t_j \leftarrow t_0}^{\tilde{\gamma}} \{ \gamma^\downarrow(t) - \gamma^\downarrow(t_j) \} \right], \quad (10.2)$$

thus Γ can be determined from Γ^\downarrow .

10.4 Expressions for manifold \mathbb{S}^d

The embedded representation of the manifold is $M = \mathbb{S}^d = \{x \in \mathbb{R}^q : x^\top x = 1\}$ for $q = d + 1$. Suppose that $p, p', x \in M$; $y \in T_p M$; and c is a geodesic curve connecting p to $p' \in M \setminus \mathcal{C}(p)$ such that $c(0) = p$ and $c(1) = p'$. Then [Absil et al., 2009, for example],

$$\begin{aligned} \exp_p^{-1}(x) &= u \{x - p \cos(u)\} / \sin(u) \in T_p M, \\ \exp_p(y) &= p \cos(\|y\|) + (y/\|y\|) \sin(y/\|y\|) \in M, \\ P_{1 \leftarrow 0}^c y &= [I_d + \{\cos(v) - 1\} w w^\top - \sin(v) p w^\top] y \in T_{p'} M, \end{aligned}$$

for $u = \cos^{-1}(p^\top x)$, $v = \cos^{-1}(p^\top p')$, $w = \{p' - p \cos(v)\} / \sin(v)$.

10.5 Expressions for manifold $\text{Sym}_{>0}(d)$.

Let $M = \text{Sym}_{>0}(r) = \{X \in \mathbb{R}^{r \times r} : X = X^\top, y^\top X y > 0, y \in \mathbb{R}^r\}$ be the positive cone of dimension $d = r(r+1)/2$ within the set of r -dimensional symmetric matrices. Suppose that $P, P', X \in M$; $Y \in T_P M$; and c is a geodesic curve connecting P to P' such that $c(0) = P$ and $c(1) = P'$. The distance from the affine-invariant metric [Pennec et al., 2019, for example] is

$$d(P, X) = \|\log(P^{-\frac{1}{2}} X P^{-\frac{1}{2}})\|,$$

and

$$\begin{aligned} \exp_P^{-1}(X) &= P^{1/2} \log\left(P^{-1/2} X P^{-1/2}\right) P^{1/2} \in T_P M, \\ \exp_P(Y) &= P^{1/2} \exp\left(P^{-1/2} Y P^{-1/2}\right) P^{1/2} \in M, \\ P_{1 \leftarrow 0}^c Y &= E Y E^\top \in T_{P'} M, \end{aligned}$$

with $E = (P' P^{-1})^{1/2}$ [Sra and Hosseini, 2015], and \log and \exp are the matrix logarithm and exponential.

10.6 Proofs

10.6.1 Proof of Theorem 3.3

For every t , suppose $F(y) := E\{\rho^2(y, x(t))\} < \infty$ at a point y , and hence on all M . For part (i), when every point $p \in M$ has empty cut locus the function $y \mapsto F(y)$ is geodesically convex on M with a global minimizer that is the unique stationary point, and the Fréchet mean of $x(t)$ is hence unique [e.g. Afsari, 2011]. On such M , $\exp_{\gamma(t)} : T_{\gamma(t)} M \rightarrow M$ is bijective, and it is thus sufficient to show that $E\{\exp_{\gamma(t)}^{-1}(x(t))\} = 0$ [e.g. Le, 2001]. Since $\exp_{\gamma(t)}^{-1}(x(t)) = P_{t \leftarrow 0}^\gamma P_{1 \leftarrow 0}^c \{y(t) - \tilde{m}(t)\}$, and the parallel transports are linear isometries, the result follows since $E\{y(t) - \tilde{m}(t)\} = 0$.

For part (ii) note that the function F defined above may be written as

$$F(y) = \int_M \rho^2(y, x(t)) d(\exp_{\gamma(t)})_{\#} \lambda(x(t)) = \int_M \rho^2(\sigma_{\gamma(t)}(y), \sigma_{\gamma(t)}(x(t))) d(\exp_{\gamma(t)})_{\#} \lambda(x(t)),$$

since M is symmetric and $\sigma_{\gamma(t)}$ is an isometry on M . Let $v \in T_{\gamma(t)} M$ be such that $\exp_{\gamma(t)}(v) = x(t)$. Since the distribution of $x(t)$ is assumed to possess even symmetry, it is of the form $(\exp_{\gamma(t)})_{\#} \lambda$ of a distribution λ with Lebesgue-density f that is symmetric around the origin in $T_{\gamma(t)} M$ such that $f(v) = f(-v)$; this holds regardless of whether v is unique when $x(t) \notin \mathcal{C}(\gamma(t))$ or a measurable selection is made from the set of all v such that $\exp_{\gamma(t)}(v) = x(t)$. Since the isometry $\sigma_{\gamma(t)}$ reverses geodesics through $\gamma(t)$, we have the relation $\exp_{\gamma(t)}(-v) = \sigma_{\gamma(t)}(\exp_{\gamma(t)}(v))$. Therefore,

$$\begin{aligned} F(y) &= \int_M \rho^2(\sigma_{\gamma(t)}(y), \sigma_{\gamma(t)}(x(t))) d(\exp_{\gamma(t)})_{\#} \lambda(x(t)) \\ &= \int_M \rho^2(\sigma_{\gamma(t)}(y), \sigma_{\gamma(t)}(x(t))) d(\exp_{\gamma(t)})_{\#} \lambda(\sigma_{\gamma(t)}(x(t))) \\ &= F(\sigma_{\gamma(t)}(y)), \end{aligned}$$

and $F : M \rightarrow \mathbb{R}$ is symmetric about $\gamma(t)$.

We now establish that it suffices to show that $\gamma(t)$ is the stationary point of F in order for it to be the Fréchet mean. Assume otherwise, and let $\gamma(t)$ be a stationary point of F whose unique minimizer is q distinct from $\gamma(t)$. Since F is symmetric about $\gamma(t)$, we have then that $\sigma_{\gamma(t)}(q)$ must also minimize F , which contradicts the uniqueness assumption of the Fréchet mean, unless $q = \sigma_{\gamma(t)}(q)$. This cannot happen since by assumption $q \notin \mathcal{C}(\gamma(t))$. The reasoning from proof of (i) can be reused to show that $\gamma(t)$ is a stationary point of F , and complete the proof.

10.6.2 Proof of Proposition 3.1

For every t , note that $y_b(t) \sim N_d(\tilde{m}(t), \tilde{k}(t, t))$. For every t , the orthonormal frame $E^\gamma(t) : T_{\gamma(0)}M \rightarrow T_{\gamma(t)}M$ is a linear operator. Consequently,

$$V^\gamma(t) \sim N_d\left(E^\gamma(t)\tilde{m}(t), E^\gamma(t)\tilde{k}(t, t)E^\gamma(t)^\top\right)$$

with values in the vector space $(T_{\gamma(t)}M, \langle \cdot, \cdot \rangle_{\gamma(t)})$, where $E^\gamma(t)^\top$ is the corresponding adjoint operator. Consider for distinct times t, t' the random vector $(V^\gamma(t), V^\gamma(t'))$ with values in the direct sum inner product space $(T_{\gamma(t)}M \oplus T_{\gamma(t')}M, \langle \cdot, \cdot \rangle_{\gamma(t)} + \langle \cdot, \cdot \rangle_{\gamma(t')})$. From the argument above it is clear that $(V^\gamma(t), V^\gamma(t'))$ is Gaussian, and that its mean is $(E^\gamma(t)\tilde{m}(t), E^\gamma(t')\tilde{m}(t'))$. From Appendix 10.1 we observe that the covariance between $V^\gamma(t)$ and $V^\gamma(t')$ is given by linear operator $\Omega_{tt'} : T_{\gamma(t)}M \oplus T_{\gamma(t')}M \rightarrow T_{\gamma(t)}M \oplus T_{\gamma(t')}M$ defined by

$$\begin{pmatrix} \Omega_{tt} & \Omega_{tt'} \\ \Omega_{tt'}^\top & \Omega_{t't'} \end{pmatrix},$$

where $\Omega_{ab} := E^\gamma(a)\tilde{k}(a, b)E^\gamma(b)^\top$. The discussion above holds for any curve γ , and thus for $\gamma = \tilde{m}_b^\uparrow$.

It is now straightforward to extend the above to the case of r times t_1, \dots, t_r involving a direct sum of r tangent spaces and corresponding $r \times r$ block covariance operator comprising $\binom{r}{2}$ linear operators $\Omega_{t_i t_j}$ for $i, j = 1, \dots, r$. This establishes the existence of finite-dimensional marginal Gaussian distributions corresponding to the choices m and k . If the family of finite-dimensional marginal distributions constitutes a *projective* family, existence and uniqueness of a Gaussian vector field $t \mapsto V^\gamma(t)$ along γ follows from Kolmogorov's extension theorem [e.g., Bhattacharya and Waymire, 2007]. Proof of projectivity follows straightforwardly from Proposition 16 in Hutchinson et al. [2021], who consider general Gaussian vector fields not necessarily along curves γ .

10.6.3 Proof of Proposition 3.2

Given a mean function m and the kernel k for the \mathbb{R}^d -valued Gaussian process z , the pair (b, U) determines $\tilde{m} = Um$ and $\tilde{k} = UkU^\top$ in T_bM , the mean and kernel, respectively, of the Gaussian process $y_b(t)$ in T_bM ; the unique rolling of \tilde{m} onto M then results in \tilde{m}_b^\uparrow . Upon setting $\gamma = \tilde{m}_b^\uparrow$, the Gaussian vector field $V^\gamma(t)$ is obtained by action of the frame $E^\gamma(t)$, determined by $E^\gamma(0) = (P_{1 \leftarrow 0}^c u_1, \dots, P_{1 \leftarrow 0}^c u_d)$, on the Gaussian process $y_b(t)$; in other words, on T_bM , the map $(U, m, k) \rightarrow V^\gamma$ is injective. The curve x on M is then defined as $x(t) = \exp_{\gamma(t)}(V^\gamma(t))$.

Choose another point $b' \in M$ with basis U' for $T_{b'}M$, resulting in the process x' on M . From the discussion above, x' will have the same distribution as x if m' and k' can be chosen such that the parallel transport of $U'm'$ and $U'k'U'^\top$ to T_bM coincides with $\tilde{m} = Um$ and $\tilde{k} = UkU^\top$. The isometric parallel transport map $P_{1 \leftarrow 0}^\eta : T_{b'}M \rightarrow T_bM$ along a curve $\eta : [0, 1] \rightarrow M$ connecting b' and b ensures that $P_{1 \leftarrow 0}^\eta U'$ is an orthonormal basis on T_bM . Thus choosing $m' := (P_{1 \leftarrow 0}^\eta U')^{-1}Um = U'^\top P_{0 \leftarrow 1}^\eta Um$ in \mathbb{R}^d gives us the desired result; a similar argument applies for k' as well. The chosen m' and k' are unique, since the parallel vector fields along η determined by U and U' that generate the parallel transport maps, respectively, from $T_{b'}M$ to T_bM and vice versa are unique. If η is chosen to be the piecewise curve consisting of a segment connecting b' to $\gamma(0)$ then a segment connecting $\gamma(0)$ to b then the result follows.

10.6.4 Proof of Proposition 4.1

The j th column of $H(X; \Gamma)$ and $H'(X; \Gamma)$, by Definition 4.1, respectively equal

$$U^\top \left[\exp_b^{-1} \{\gamma(0)\} + P_{0 \leftarrow 1}^c \gamma^\downarrow(t_j) + P_{0 \leftarrow 1}^c P_{0 \leftarrow t_j}^\gamma \exp_{\gamma(t_j)}^{-1} \{x(t_j)\} \right]; \quad (10.3)$$

$$U'^\top \left[\exp_{b'}^{-1} \{\gamma(0)\} + P_{0 \leftarrow 1}^{c'} \gamma^\downarrow(t_j) + P_{0 \leftarrow 1}^{c'} P_{0 \leftarrow t_j}^{\gamma'} \exp_{\gamma(t_j)}^{-1} \{x(t_j)\} \right]. \quad (10.4)$$

Direct substitution shows that left-multiplying the former by $A = (U')^\top P_{0 \leftarrow 1}^{c'} P_{1 \leftarrow 0}^c (U^\top)^{-1}$ and adding $a = (U')^\top \left[\exp_{b'}^{-1} \{\gamma(0)\} - P_{0 \leftarrow 1}^{c'} P_{1 \leftarrow 0}^c (U^\top)^{-1} \exp_b^{-1} \{\gamma(0)\} \right]$ leads to the latter. Hence $H'(X_i; \Gamma) = a 1_r^\top + AH(X_i; \Gamma) \sim \mathcal{MN}(a 1_r^\top + AM_w \Phi, AU_w A^\top, \Phi^\top V_w \Phi)$; and the result follows by writing $1_r^\top = 1_k^\top \Phi$, using that the constant function is in the span of Φ . The a and A specific to the result can be computed from the expressions above, with $\gamma(0) = \exp_b \{M_w \phi(t_1)\}$.

10.6.5 Proof of Proposition 4.2

The solution to (4.10) is $\hat{M}_w^{\text{Fre}} = \frac{1}{n} \sum_{i=1}^n H(X_i; \hat{\Gamma}_{\text{Fre}}) \Phi^-$. The j th column of $H(X_i; \hat{\Gamma}_{\text{Fre}})$ is

$$U^\top \left[(\hat{\gamma}_{\text{Fre}})_b^\downarrow(t_j) + P_{0 \leftarrow 1}^c P_{0 \leftarrow t_j}^{\hat{\gamma}_{\text{Fre}}} \exp_{\hat{\gamma}_{\text{Fre}}(t_j)}^{-1} \{x_i(t_j)\} \right], \quad (10.5)$$

and by definition of the sample Fréchet mean, $\hat{\gamma}_{\text{Fre}}$, for every j ,

$$\frac{1}{n} \sum_{i=1}^n \exp_{\hat{\gamma}_{\text{Fre}}(t_j)}^{-1} \{x_i(t_j)\} = 0 \in T_{\hat{\gamma}_{\text{Fre}}(t_j)} M. \quad (10.6)$$

Thus, using (10.5) and (10.6), and that the parallel transports are linear isometries, we have that

$$\hat{M}_w^{\text{Fre}} = \frac{1}{n} \sum_{i=1}^n H(X_i; \hat{\Gamma}_{\text{Fre}}) \Phi^- = U^\top (\hat{\Gamma}_{\text{Fre}})_b^\downarrow \Phi^- = H(\hat{\Gamma}_{\text{Fre}}; \hat{\Gamma}_{\text{Fre}}) \Phi^-.$$

10.6.6 Proof of Theorem 4.2

The proof requires convergence of parallel transport maps along the sample Fréchet mean curve to parallel transport maps along the population Fréchet mean curve. This is recorded in the following Lemma, which is stated generally and may be of independent interest. The Lemma uses the notion of C^1 curves on M and their convergence in the weak C^1 topology, to be understood in local coordinates: given a chart (U, ψ) with open $U \subset M$ and smooth $\psi : U \rightarrow V$, where V is an open subset of \mathbb{R}^d , the coordinate representative of a curve $c : [0, 1] \rightarrow M$ is the Euclidean curve $\tilde{c} = \psi \circ c$. Then c is a C^1 curve if \tilde{c} is C^1 with respect to the norm $\|\tilde{c}\|_{C^1} := \sup_t \|\tilde{c}(t)\| + \sup_t \|\dot{\tilde{c}}(t)\|$; see Hirsch [2012, Chapter 2] for details.

Lemma 10.2. *Let γ_n be a sequence of C^1 curves on M that converge in probability to a deterministic curve γ in the weak C^1 topology. Then, parallel vector fields along γ_n converge in probability to parallel vector fields along γ .*

Proof. For every n , a parallel vector field V_n along γ_n is the solution to the initial-value, first-order linear ordinary differential equation

$$\begin{aligned} \dot{V}_n(t) &= -A(\gamma_n(t))V_n(t), \quad 0 < t \leq 1, \\ V_n(0) &= v_n, \end{aligned}$$

where, in local coordinates using the summation notation, $A^k(\gamma_n(t)) := \dot{\gamma}_n^i(t)\Gamma_{ij}^k(\gamma_n(t))$, and Γ_{ij}^k are the Christofel symbols [p. 106 Lee, 2018]; a parallel vector field V along γ satisfies a similar system of differential equations with coefficient $A(\gamma)$ and initial condition $V(0) = v$. The coefficient A in the differential equations is constant in V_n and V , and the map $M \rightarrow TM$ is continuous, since γ_n and γ are assumed to be continuously differentiable, and the Christoffel symbols $x \mapsto \Gamma_{ij}^k(x)$ are continuous on M for each coordinate k ; in a compact set within any chart, it is bounded.

Suppose γ lies in a single chart. Then, since γ_n are converging to γ , for a large enough n , we may assume that γ_n , for all n , and γ lie in the same chart. Using the reasoning above, we note the solutions may be written in the integral form

$$V_n(t) = V_n(0) - \int_0^t A(\gamma_n(s))V_n(s)ds, \quad V(t) = V(0) - \int_0^t A(\gamma(s))V(s)ds.$$

Then, the deviation $E_n(t) := V_n(t) - V(t)$ is expressed as

$$\begin{aligned} E_n(t) &= V_n(0) - V(0) - \int_0^t A(\gamma_n(s))V_n(s)ds + \int_0^t A(\gamma(s))V(s)ds \\ &= V_n(0) - V(0) \\ &\quad - \int_0^t A(\gamma_n(s))V_n(s)ds + \int_0^t A(\gamma_n(s))V(s)ds - \int_0^t A(\gamma_n(s))V(s)ds + \int_0^t A(\gamma(s))V_n(s)ds \\ &= [V_n(0) - V(0)] - \int_0^t A(\gamma_n(s)) [V_n(s) - V(s)] ds + \int_0^t [A(\gamma(s)) - A(\gamma_n(s))] V(s)ds. \end{aligned}$$

Using $\|\cdot\|$ to generically refer to norm $\|\cdot\|_x$ on T_xM coming from the inner product, we obtain

$$\begin{aligned} \|E_n(t)\| &\leq \|V_n(0) - V(0)\| + \int_0^t \|E_n(s)\| \|A(\gamma_n(s))\| ds + \int_0^t \|A(\gamma_n(s)) - A(\gamma(s))\| \|V(s)\| ds \\ &= (a) + (b) + (c) \end{aligned}$$

The term (a) converges in probability to zero since $\dot{\gamma}_n \xrightarrow{P} \dot{\gamma}$ uniformly in t , under the assumption of C^1 convergence. For term (c), note that the vector field $t \mapsto V(t)$, as a solution to a linear first-order differential equation, is continuous and has a finite upper bound $L := \sup_t \|V(t)\|$ on an interval. Using the properties of the coefficient A discussed above, for a large enough n and $\epsilon > 0$, (c) satisfies

$$\int_0^t \|A(\gamma_n(s)) - A(\gamma(s))\| \|V(s)\| ds \leq \epsilon L.$$

Using Gronwall's inequality, we obtain

$$\|E_n(t)\| \leq \epsilon L \exp \left\{ \int_0^t \|A(\gamma_n(s))\| ds \right\} + o_p(1).$$

Since $\epsilon \rightarrow 0$ as $n \rightarrow \infty$, we are done. When γ is not covered by a single chart, we can use the reasoning used in proof of Theorem 4.32 in Lee [2018], on uniqueness of the parallel vector field V along γ with initial condition $V(0) = v$, to suitably modify the preceding arguments. \square

Proof. Convergence in probability of $\hat{\gamma}_{\text{Fre}}$ in the C^1 topology to γ implies convergence for any finite number of times t_1, \dots, t_m , so that $\hat{\Gamma}_{\text{Fre}}$ converges in probability to Γ as $n \rightarrow \infty$. Note that from (4.2),

$$H(\hat{\Gamma}_{\text{Fre}}; \hat{\Gamma}_{\text{Fre}}) = U^\top \left\{ (\hat{\gamma}_{\text{Fre}})^\downarrow_b(t_1) + P_{0 \leftarrow 1}^c P_{0 \leftarrow t_1}^{\hat{\gamma}_{\text{Fre}}}(0), \dots, (\hat{\gamma}_{\text{Fre}})^\downarrow_b(t_m) + P_{0 \leftarrow 1}^c P_{0 \leftarrow t_m}^{\hat{\gamma}_{\text{Fre}}}(0) \right\},$$

since $\exp_x^{-1}(x) = 0 \in T_x M$. From Lemma 10.2, we observe that for a fixed frame U , $H(\hat{\Gamma}_{\text{Fre}}; \hat{\Gamma}_{\text{Fre}})$ converges in probability to $H(\Gamma_{\text{Fre}}, \Gamma_{\text{Fre}})$, where Γ_{Fre} is the discretization of γ_{Fre} . Then, from Theorem 3.3 we deduce that $H(\hat{\Gamma}_{\text{Fre}}, \hat{\Gamma}_{\text{Fre}})\Phi^-$ converges in probability to $H(\Gamma_{\text{Fre}}, \Gamma_{\text{Fre}})\Phi^-$ as $n \rightarrow \infty$. \square

References

- P-A Absil, Robert Mahony, and Rodolphe Sepulchre. *Optimization Algorithms on Matrix Manifolds*. Princeton University Press, 2009.
- Bijan Afsari. Riemannian L^p center of mass: existence, uniqueness, and convexity. *Proceedings of the American Mathematical Society*, 139(2):655–673, 2011.
- Rabindra Nath Bhattacharya and Edward C Waymire. *A Basic Course in Probability Theory*, volume 69. Springer, 2007.
- Xiongtao Dai and Hans-Georg Müller. Principal component analysis for functional data on Riemannian manifolds and spheres. *The Annals of Statistics*, pages 3533–3577, 2019.
- C. De Boor. *A Practical Guide to Splines*. Springer New York, 2002.
- Paromita Dubey and Hans-Georg Müller. Functional models for time-varying random objects. *Journal of the Royal Statistical Society Series B: Statistical Methodology*, 82(2):275–327, 2020.
- Paromita Dubey and Hans-Georg Müller. Modeling time-varying random objects and dynamic networks. *Journal of the American Statistical Association*, 117(540):2252–2267, 2022.
- Pierre Dutilleul. The MLE algorithm for the matrix normal distribution. *Journal of statistical computation and simulation*, 64(2):105–123, 1999.
- M. L. Eaton. *Multivariate Statistics: A Vector Space Approach*. Wiley-Blackwell, 1983.
- Morris W Hirsch. *Differential Topology*, volume 33. Springer Science & Business Media, 2012.
- Michael Hutchinson, Alexander Terenin, Viacheslav Borovitskiy, So Takao, Yee Teh, and Marc Deisenroth. Vector-valued gaussian processes on Riemannian manifolds via gauge independent projected kernels. *Advances in Neural Information Processing Systems*, 34:17160–17169, 2021.
- Peter E Jupp and John T Kent. Fitting smooth paths to spherical data. *Journal of the Royal Statistical Society Series C: Applied Statistics*, 36(1):34–46, 1987.
- Kwang-Rae Kim, Ian L Dryden, Huiling Le, and Katie E Severn. Smoothing splines on Riemannian manifolds, with applications to 3D shape space. *Journal of the Royal Statistical Society Series B: Statistical Methodology*, 83(1):108–132, 2021.
- Shoshichi Kobayashi and Katsumi Nomizu. *Foundations of Differential Geometry*, volume 2. John Wiley & Sons, 1996.
- Alfred Kume, Ian L Dryden, and Huiling Le. Shape-space smoothing splines for planar landmark data. *Biometrika*, 94(3):513–528, 2007.
- Huiling Le. Locating Fréchet means with application to shape spaces. *Advances in Applied Probability*, (2):324–338, 2001.
- John M Lee. *Introduction to Riemannian manifolds*, volume 2. Springer, 2018.

- Zhenhua Lin and Fang Yao. Intrinsic Riemannian functional data analysis. *The Annals of Statistics*, 47(6):3533–3577, 2019.
- Jinzhao Liu, Chao Liu, Jian Qing Shi, and Tom Nye. Wrapped Gaussian process functional regression model for batch data on Riemannian manifolds. *arXiv preprint arXiv:2409.03181*, 2024.
- Anton Mallasto and Aasa Feragen. Wrapped Gaussian process regression on Riemannian manifolds. In *Proceedings of the IEEE Conference on Computer Vision and Pattern Recognition*, pages 5580–5588, 2018.
- Xavier Pennec, Stefan Sommer, and Tom Fletcher. *Riemannian Geometric Statistics in Medical Image Analysis*. Academic Press, 2019.
- Michael J Prentice. Orientation statistics without parametric assumptions. *Journal of the Royal Statistical Society Series B: Statistical Methodology*, 48(2):214–222, 1986.
- R Core Team. *R: A Language and Environment for Statistical Computing*. R Foundation for Statistical Computing, Vienna, Austria, 2023. URL <https://www.R-project.org/>.
- J.O. Ramsay, G. Hooker, and S. Graves. *Functional data analysis with R and Matlab*. Springer, 2009.
- Lingxuan Shao, Zhenhua Lin, and Fang Yao. Intrinsic Riemannian functional data analysis for sparse longitudinal observations. *The Annals of Statistics*, 50(3):1696–1721, 2022.
- Richard W Sharpe. *Differential Geometry: Cartan’s Generalization of Klein’s Erlangen Program*. Springer, 2000.
- Stefan Sommer. An infinitesimal probabilistic model for principal component analysis of manifold valued data. *Sankhya A*, 81(1):37–62, 2019.
- Stefan Sommer. Probabilistic approaches to geometric statistics: Stochastic processes, transition distributions, and fiber bundle geometry. In *Riemannian Geometric Statistics in Medical Image Analysis*, pages 377–416. Elsevier, 2020.
- Suvrit Sra and Reshad Hosseini. Conic geometric optimization on the manifold of positive definite matrices. *SIAM Journal on Optimization*, 25(1):713–739, 2015.
- Jingyong Su, Sebastian Kurtek, Eric Klassen, and Anuj Srivastava. Statistical analysis of trajectories on Riemannian manifolds: bird migration, hurricane tracking and video surveillance. *The Annals of Applied Statistics*, 8(1):530–552, 2014.
- Zhanfeng Wang, Xinyu Li, and Jian Qing Shi. Intrinsic wrapped Gaussian process regression modeling for manifold-valued response variable. *arXiv preprint arXiv:2411.18989*, 2024.
- Zhengwu Zhang, Eric Klassen, and Anuj Srivastava. Phase-amplitude separation and modeling of spherical trajectories. *Journal of Computational and Graphical Statistics*, 27(1):85–97, 2018.
- Herbert Ziezold. On expected figures and a strong law of large numbers for random elements in quasi-metric spaces. In *European Meeting of Statisticians, 1974*, pages 591–602. Springer, 1977.